J Biomol NMR (2014) 59:211–217
DOI 10.1007/s10858-014-9842-2

COMMUNICATION

An approach to sequential NMR assignments of proteins: application to chemical shift restraint-based structure prediction

Christoph Wiedemann · Peter Bellstedt · Christian Herbst · Matthias Görlach · Ramadurai Ramachandran

Received: 15 April 2014 / Accepted: 10 June 2014 / Published online: 19 June 2014
© Springer Science+Business Media Dordrecht 2014

Abstract A procedure for the simultaneous acquisition of {HNCOCANH & HCCCONH} chemical shift correlation spectra employing sequential ^{1}H data acquisition for moderately sized proteins is presented. The suitability of the approach for obtaining sequential resonance assignments, including complete ^{15}N, ^{1}H^{N}, ^{13}CO, ^{13}C$^{\alpha}$, ^{13}C$^{\beta}$ and ^{1}H$^{\alpha}$ chemical shift information, is demonstrated experimentally for a ^{13}C and ^{15}N labelled sample of the C-terminal winged helix (WH) domain of the minichromosome maintenance (MCM) complex of *Sulfolobus solfataricus*. The chemical shift information obtained was used to calculate the global fold of this winged helix domain *via* CS-Rosetta. This demonstrates that our procedure provides a reliable and straight-forward protocol for a quick global fold determination of moderately-sized proteins.

Keywords Protein structure prediction · Sequential data acquisition · Protein resonance assignment · CS-Rosetta · Winged helix domain

Electronic supplementary material The online version of this article (doi:10.1007/s10858-014-9842-2) contains supplementary material, which is available to authorized users.

C. Wiedemann · P. Bellstedt · M. Görlach ·
R. Ramachandran (✉)
Biomolecular NMR Spectroscopy, Leibniz Institute for Age Research - Fritz Lipmann Institute, Beutenbergstr. 11, 07745 Jena, Germany
e-mail: raman@fli-leibniz.de

C. Herbst
Department of Physics, Ubon Ratchathani University, Ubon Ratchathani 34190, Thailand

Introduction

NMR spectroscopy constitutes a powerful technique for the elucidation of the three-dimensional structure of proteins in solution as well as in the solid state. Conventionally, solution state NMR studies mostly rely on the use of a large number of structural parameters, *e.g.* ^{1}H-^{1}H inter-nuclear distance estimates obtained from NOESY type experiments and torsion angle restraints derived from three-bond homo- and heteronuclear scalar couplings. Such information is used in structure calculation programs such as CYANA (Güntert 2004) and CNS (Brünger et al. 1998) to obtain an ensemble of structures consistent with the experimental restraints. This conventional approach, however, is time-consuming and critically depends on the reliability and the number of assigned NOE crosspeaks in determining accurate structures. On the other hand, efficient computational procedures, such as CS-Rosetta (Shen et al. 2008; Lange et al. 2012), have been developed in recent years to accurately predict protein structures. Conformationally sensitive backbone and side chain chemical shifts, that are obtained during the course of the resonance assignment process, are used as restraints in these NMR-assisted computational procedures to efficiently search the conformational space for the protein structures with the lowest energy. Here, we present, in continuation of our recent studies (Bellstedt et al. 2014; Wiedemann et al. 2014), an approach to obtain in one-shot sequential backbone and side chain resonance assignments in moderately sized proteins *via* the simultaneous acquisition of {HNCOCANH (Shirakawa et al. 1995; Bracken et al. 1997) & HCCCONH (Logan et al. 1992; Clowes et al. 1993; Zuiderweg et al. 1996; Carlomagno et al. 1996)} chemical shift correlation spectra employing a sequential ^{1}H data acquisition procedure.

The suitability of this approach for obtaining ^{15}N, ^{1}H^{N}, ^{13}CO, ^{13}C$^{\alpha}$, ^{13}C$^{\beta}$ and ^{1}H$^{\alpha}$ chemical shifts is experimentally demonstrated using a [^{13}C, ^{15}N]-labelled sample of the C-terminal winged helix (WH) domain of the mini-chromosome maintenance (MCM) complex of *Sulfolobus solfataricus*, a 82 amino acid residue protein domain that is currently under investigation in our laboratory (Wiedemann et al. 2013). The global fold of the protein as determined *via* CS-Rosetta using the backbone and side chain chemical shift restraints is also presented.

Materials and methods

NMR experiments were carried out on a 750 MHz narrow-bore Avance III NMR spectrometer equipped with pulse field gradient accessories, pulse shaping units and a triple resonance cryoprobe and with the sample temperature kept at 303 K. Homonuclear in-phase magnetisation transfers were achieved using amplitude and phase-modulated mixing sequences (AK2-JCC and AK4-JC$^{\alpha}$CO$_{aniso}$; Kirschstein et al. 2008a, b). The States procedure was used for phase-sensitive detection in the indirect dimensions (States et al. 1982). Signals arising from different magnetisation transfer pathways of interest were selected by standard phase cycling procedures. The samples were a 1 mM (Suppl. Material Figure S5 and S6) and 7 mM uniformly ^{13}C, ^{15}N-labelled *Sulfolobus solfataricus* MCM C-terminal WH domain. DSS was used for direct ^{1}H chemical shift referencing and ^{13}C and ^{15}N chemical shifts were indirectly referenced. Frequency switching in the ^{13}C and ^{1}H channels were carried out, where needed, while the respective magnetisation was along the z-axis.

The resolution-adapted structural recombination (RASREC) protocol (Raman et al. 2010; Lange and Baker 2012; Schot et al. 2013) of the chemical-shift restraint Rosetta NMR structure calculation suite (Shen et al. 2008; Lange et al. 2012) was used to calculate a pool of NMR structures only based on the amino acid sequence and chemical shifts obtained from the one-shot NMR experiment described in this study. The CS-Rosetta suite 3.0 with the Rosetta version 3.4 and the toolbox version 1.4 was used. The number of confomers that were used in the global structure pool was 100 and no chemical shift rescoring was applied to the structures in the pool. Flexible parts of the N-terminus (E605-I609) as predicted by TALOS+ (Shen et al. 2009) were excluded from structure calculations. The calculation was performed on a Linux operated computer equipped with four 10-core Intel Xeon E7- 4870 (2.40 GHz) processors (80 logical CPUs) and required 26 h.

Results and discussion

The triple resonance HNCOCANH and HCCCONH experiments involve, respectively, the magnetisation transfer pathways $^{1}H^{N}\rightarrow{}^{15}N\rightarrow{}^{13}CO\rightarrow{}^{13}C^{\alpha}\rightarrow{}^{15}N\rightarrow{}^{1}H^{N}$ and $^{1}H^{sc}\rightarrow{}^{13}C^{sc}\rightarrow{}^{13}C^{\alpha}\rightarrow{}^{13}CO\rightarrow{}^{15}N\rightarrow{}^{1}H^{N}$. The extraction of all the ^{15}N, ^{1}H^{N}, ^{13}CO, ^{13}C$^{\alpha}$, ^{13}C$^{\beta}$ and ^{1}H$^{\alpha}$ chemical shifts can be achieved either together by the simultaneous acquisition of two 4D experiments, H(N)CO(CA)NH and HC(CCO)NH, or, as we present here, by carrying out two experiments involving the sequential collection of two 3D spectra:

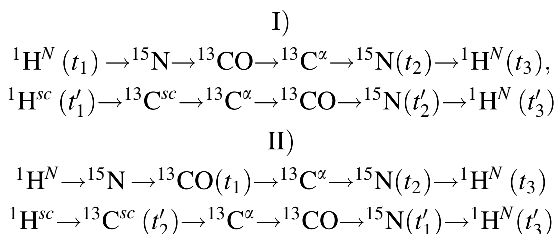

I)

$$^{1}H^{N}(t_1)\rightarrow{}^{15}N\rightarrow{}^{13}CO\rightarrow{}^{13}C^{\alpha}\rightarrow{}^{15}N(t_2)\rightarrow{}^{1}H^{N}(t_3),$$
$$^{1}H^{sc}(t_1')\rightarrow{}^{13}C^{sc}\rightarrow{}^{13}C^{\alpha}\rightarrow{}^{13}CO\rightarrow{}^{15}N(t_2')\rightarrow{}^{1}H^{N}(t_3')$$

II)

$$^{1}H^{N}\rightarrow{}^{15}N\rightarrow{}^{13}CO(t_1)\rightarrow{}^{13}C^{\alpha}\rightarrow{}^{15}N(t_2)\rightarrow{}^{1}H^{N}(t_3)$$
$$^{1}H^{sc}\rightarrow{}^{13}C^{sc}(t_2')\rightarrow{}^{13}C^{\alpha}\rightarrow{}^{13}CO\rightarrow{}^{15}N(t_1')\rightarrow{}^{1}H^{N}(t_3')$$

The RF pulse scheme for the recording of the 3D H(NCOCA)NH and H(CCCO)NH data sets *via* sequential ^{1}H data acquisition is shown in Fig. 1a. The initial transverse magnetisation generated from both ^{15}N and ^{13}C attached protons by the first 90° pulse is allowed to undergo chemical shift evolution during the t_1/t_1' period. These evolve under the one bond heteronuclear $^{15}N-{}^{1}H$ and $^{13}C-{}^{1}H$ scalar couplings during the periods $2\Delta_0$ and $(\Delta_0+\Delta_1-\Delta_2)$, respectively, to generate the relevant antiphase ^{1}H magnetisations. The antiphase ^{1}H magnetisations are then converted into the corresponding antiphase nitrogen and carbon magnetisations by the 90° pulses applied to the different nuclei. The antiphase ^{15}N and ^{13}C polarisations are then allowed to refocus during the interval $2\tau_1$ and $2\tau_2$ and flipped to the z-axis to generate $(^{15}N/^{13}C)^{z}$ magnetisation. The $(^{13}C^{sc})^{z}$ magnetisation is first subjected to a period of $^{13}C-{}^{13}C$ longitudinal TOCSY mixing, keeping the ^{13}C RF carrier at the middle of the aliphatics spectral range (35 ppm), to generate $(^{13}C^{\alpha})^{z}$ magnetisation. The ^{13}C$^{\alpha}$ magnetisation is then brought to the transverse plane and subjected to a period of $^{13}C^{\alpha}\rightarrow{}^{13}CO$ anisotropic cross polarisation, while keeping the ^{13}C RF carrier at an intermediate frequency of 115 ppm. The transverse ^{13}CO magnetisation is then flipped to the z-state and the ^{13}C RF frequency switched to the ^{13}CO chemical shift position of 175 ppm. The ^{13}CO and ^{15}N magnetisation is subsequently brought to the transverse plane followed by a period of $^{13}CO\leftrightarrow{}^{15}N$ magnetisation exchange *via* the application of a band-selective INEPT (Morris and Freeman 1979) mixing sequence. The transverse ^{15}N and ^{13}CO magnetisation arising *via* $^{13}CO\rightarrow{}^{15}N$ and $^{15}N\rightarrow{}^{13}CO$ transfers at the end

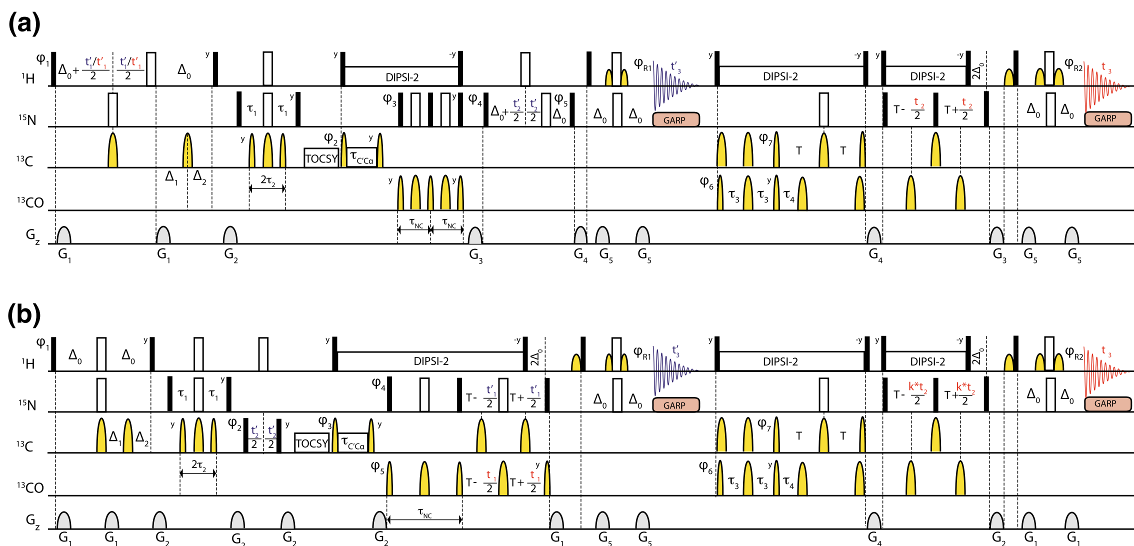

Fig. 1 RF pulse schemes for the simultaneous acquisition of (**a**) 3D H(CCCO)NH and 3D H(NCOCA)NH (**b**) 3D (H)C(CCO)NH and 3D (HN)CO(CA)NH chemical shift correlation spectra with dual sequential ^{1}H acquisitions in the direct dimension. Delay durations are as follows: $\Delta_{0,1,2} = 2.58, 1.58, 1.0\,\text{ms}$, $2\tau_1 = 2\Delta_0$, $2\tau_2 = 4\,\text{ms}$, $\tau_3 = 3.6\,\text{ms}$, $\tau_4 = 4.4\,\text{ms}, \text{T} = 12.4\,\text{ms}$, $\tau_{NC} = 25.5\,\text{ms}$. Phase cycling is as follows: (**a**) $\phi_1 = \text{x}, -\text{x}$; $\phi_2 = 8(\text{y}), 8(\text{-y})$; $\phi_3 = \phi_4 = 4(\text{y}), 4(\text{-y})$; $\phi_5 = \phi_6 = 2(\text{x}), 2(-\text{x})$; $\phi_7 = 8(\text{x}), 8(-\text{x})$; $\phi_{R1} = \phi_{R2} = \text{x}, 2(-\text{x}), \text{x}, -\text{x}, 2(\text{x}), 2(-\text{x}), 2(\text{x}), -\text{x}, \text{x}, 2(-\text{x}), \text{x}$. (**b**) $\phi_1 = \text{x}, \text{-x}$; $\phi_2 = \phi_4 = 4(\text{y}), 4(-\text{y})$; $\phi_3 = 8(\text{y}), 8(-\text{y})$; $\phi_5 = 2(\text{y}), 2(-\text{y})$; $\phi_6 = 2(\text{x}), 2(-\text{x})$; $\phi_7 = 8(\text{x}), 8(-\text{x})$; $\phi_{R1} = \phi_{R2} = \text{x}, 2(-\text{x}), \text{x}, -\text{x}, 2(\text{x}), 2(-\text{x}), 2(\text{x}), -\text{x}, \text{x}, 2(-\text{x}), \text{x}$. Gradients with a sine bell amplitude profile were used. Durations and strengths (as % of the 50 G/cm maximum strenghth) are $\text{G}_1 = 1\,\text{ms}$ (50 %), $\text{G}_2 = 5\,\text{ms}$ (50 %), $\text{G}_3 = 5\,\text{ms}$ (80 %), $\text{G}_4 = 1\,\text{ms}$ (60 %), $\text{G}_5 = 1\,\text{ms}$ (80 %), respectively. Open and filled rectangles represent 180° and 90° hard pulses, respectively. Shaped 180° and 90° pulses were used for band-selective ^{13}C excitation. Where required frequency switching in the ^{13}C and ^{1}H channels were carried out while the respective magnetisation was along the z-axis

of the INEPT step are flipped to the z axis. The ^{15}N magnetisation generated *via* the $^{13}\text{CO}{\to}^{15}\text{N}$ transfer is first allowed to evolve under its chemical shift during the t_2' period and transferred to the attached proton *via* an INEPT step and observed in the t_3' period, using the WATERGATE sequence for water suppression and under ^{15}N decoupling, to generate the 3D H(CCCO)NH spectrum.

After the completion the first ^{1}H acquisition, the ^{13}CO magnetisation arising *via* the $^{15}\text{N} \to {}^{13}\text{CO}$ transfer step is brought to the transverse plane and subjected to a series of INEPT type polarisation transfers *via* the pathway $^{13}\text{CO} \to {}^{13}\text{C}^{\alpha} \to {}^{15}\text{N} \to {}^{1}\text{H}^{N}$, as per well established procedures. The transverse ^{15}N magnetisation generated during this process is chemical shift labelled (t_2) during a constant time evolution period. The ^{1}H signals at the end are acquired in t_3, under ^{15}N decoupling and employing the WATERGATE sequence for water suppression, to generate the 3D H(NCOCA)NH spectrum. Signals arising *via* different pathways in the two sequentially collected data sets are selected by standard phase cycling procedures and by application of appropriate field gradient pulses. Note that in the H(NCOCA)NH data set, due to the presence of $^1\text{J}_{C\alpha N}$ and $^2\text{J}_{C\alpha N}$ couplings, cross- and diagonal-peaks in the H(NCOCA)NH spectrum appear *via* magnetisation transfer pathways such as:

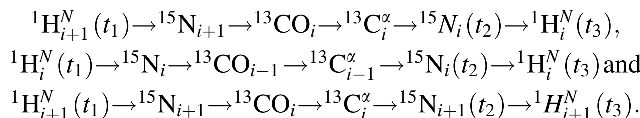

H(NCOCA)NH

$$^1\text{H}^N_{i+1}(t_1)\to{}^{15}\text{N}_{i+1}\to{}^{13}\text{CO}_i\to{}^{13}\text{C}^{\alpha}_i\to{}^{15}N_i(t_2)\to{}^1\text{H}^N_i(t_3),$$
$$^1\text{H}^N_i(t_1)\to{}^{15}\text{N}_i\to{}^{13}\text{CO}_{i-1}\to{}^{13}\text{C}^{\alpha}_{i-1}\to{}^{15}\text{N}_i(t_2)\to{}^1\text{H}^N_i(t_3)\,\text{and}$$
$$^1\text{H}^N_{i+1}(t_1)\to{}^{15}\text{N}_{i+1}\to{}^{13}\text{CO}_i\to{}^{13}\text{C}^{\alpha}_i\to{}^{15}\text{N}_{i+1}(t_2)\to{}^1H^N_{i+1}(t_3).$$

In the H(CCCO)NH experiment, starting from the side chain $^1\text{H}^{sc}$ spins of residue (i-1), inter-residue crosspeaks arise *via* the magnetisation transfer pathway:

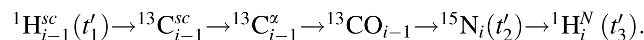

H(CCCO)NH

$$^1\text{H}^{sc}_{i-1}(t_1')\to{}^{13}\text{C}^{sc}_{i-1}\to{}^{13}\text{C}^{\alpha}_{i-1}\to{}^{13}\text{CO}_{i-1}\to{}^{15}\text{N}_i(t_2')\to{}^1\text{H}^N_i(t_3').$$

The RF pulse scheme for the one-shot collection of the 3D (HN)CO(CA)NH and (H)C(CCO)NH data sets *via* sequential ^{1}H data acquisitions, Fig. 1b, is essentially the same as that shown in Fig. 1a except for some minor changes incorporated to achieve the desired ^{13}CO and $^{13}\text{C}^{sc}$ chemical shift evolution. The transverse ^{15}N and ^{13}CO magnetisations arising *via* $^{13}\text{CO}{\to}^{15}\text{N}$ and $^{15}\text{N}{\to}^{13}\text{CO}$ transfers are chemical shift encoded simultaneously during the second constant time period, 2T, of the INEPT ^{15}N and ^{13}CO mixing step. The ^{15}N magnetisation generated *via* the $^{13}\text{CO}{\to}^{15}\text{N}$ transfer is first transferred to the attached proton through the INEPT scheme and observed in t_3'. This is then followed, as before, by a series of INEPT type

polarisation transfers to observe the signal arising *via* the pathway $^{13}CO \rightarrow {}^{13}C^{\alpha} \rightarrow {}^{15}N \rightarrow {}^{1}H^{N}$. Note that the spectral widths in the corresponding indirect t_2/t_2' dimensions in the two data sets can be independently adjusted by appropriate scaling of the increments and that spectral folding in one data set does not lead to resonance overlaps in the other, as two independent data sets are being acquired. The availability of both the H(NCOCA)NH and (HN)CO(CA)NH data sets and the presence of cross-peaks arising *via* both $^{1}J_{C\alpha N}$ and $^{2}J_{C\alpha N}$ couplings makes it possible to establish unambiguous direct connectivities between sequential amide groups.

An analysis of the cross- and diagonal peak coordinates in the $\omega_1 - \omega_3$ planes taken at different chemical shift positions of the ^{15}N dimension (ω_2) in the H(NCOCA)NH spectrum permits the identification of the adjacent $^{15}N_i$ and $^{15}N_{i+1}$ nuclei as the $\omega_1 - \omega_3$ planes taken at these ^{15}N positions would have a peak that has the same ω_1 coordinate, corresponding to that of the $^{1}H^{N}_{i+1}$, in both the planes. Any ambiguity in the correct identification of the adjacent $^{15}N_i$ and $^{15}N_{i+1}$ nuclei can easily be resolved by an inspection of the 3D (HN)CO(CA)NH spectrum. The $\omega_1 - \omega_3$ planes taken at the $^{15}N_i$ and $^{15}N_{i+1}$ chemical shift positions in this spectrum would have a set of peaks that exhibit the same ω_1 coordinates, corresponding to that of the $^{13}CO_i$, in both the planes. With the amino acid type information obtained from ^{13}C side chain chemical shifts for residues such as glycine, threonine and serine, the acquisition of 3D HNCOCANH and HCCCONH data sets permits, as shown in Figs. 2 and 3, the unambiguous sequential resonance assignments of the majority of the back bone ^{15}N, $^{13}C^{\alpha}$, ^{13}CO and $^{1}H^{N}$ as well as the side chain ^{1}H and ^{13}C nuclei in the fully protonated protein system investigated here. 1D spectral cross sections taken from the 2D slices (Figs. 2c,d, 3c,d) and spectra collected from a 1 mM sample of MCM C-terminal WH domain are given for further information (Suppl. Material). The assigned chemical shifts obtained from the presented experiments (Suppl. Material Tab. 1) are consistent with the data reported previously (BMRB entry 18986) and were used to generate structural models using the CS-Rosetta program. Figure 4 presents a superposition of the backbone ribbon representations of ten lowest energy CS-Rosetta structures of the C-terminal winged helix (WH) domain of the minichromosome maintenance (MCM) complex of *Sulfolobus solfataricus*. The chemical shift generated structural models adopt a winged helix fold of three α-helices and three β-strands in the order h1-s1-h2-h3-s2-s3 (see also Figure S7). The CS-Rosetta generated models fit the NOE-based solution structure (PDB: 2M45) reasonably well with a backbone rmsd of 1.84 Å (Figure S7).

The results presented here clearly show that it is possible, using only INEPT-type $^{15}N-^{13}C$ magnetisation transfers and sequential ^{1}H data acquisition procedure, to implement efficient RF pulse schemes for the simultaneous acquisition of triple resonance chemical shift correlation spectra such as {HNCOCANH & HCCCONH} and to obtain at the same time sequential resonance assignments and chemical shifts, including that of the backbone ^{13}CO, that are typically used as restraints in protein structure prediction programs such as CS-Rosetta.

The NMR pulse schemes presented here were developed for moderately-sized protein. In such systems the relaxation losses during ^{15}N-^{13}C mixing periods are not expected to be significant even in a fully protonated sample. Yet, NMR investigations on large proteins would typically require ^{2}H-labelled samples to minimise relaxation losses (Grzesiek et al. 1993; Yamazaki et al. 1994). Since only amide proton detection is involved in the direct dimension, the RF pulse schemes reported here can easily be adapted for the simultaneous acquisition of correlation spectra such as {HNCOCANH & CCCONH} to obtain resonance assignments and chemical shift data of larger $[^{2}H, ^{13}C, ^{15}N]$-labelled protein molecules in a protonated solvent with direct ^{13}C excitation of sidechain resonances (Farmer and Venters 1995; Venters et al. 1996) which is, however, less sensitive than direct ^{1}H excitation.

Compared to running two separate experiments the reduction in the overall time in the sequential data acquisition approach arises by avoiding one recycle delay. However, the savings in time is determined by the acquisition times employed in the indirect and direct dimensions, t_2' and t_3', respectively. Considering that we have employed shortened t_2' and t_3' acquisition times, it is possible to achieve essentially a factor of ~ 2 savings in time by sequentially collecting two data sets. Unlike in a stand alone experiment, in the sequentially acquired H(NCOCA)NH experiment, the ^{15}N and ^{13}CO magnetisations are kept along the z-axis for short periods before effecting the $^{15}N \rightarrow {}^{13}CO$ and $^{13}CO \rightarrow {}^{13}C^{\alpha}$ magnetisation transfers. However, with short residence time of the ^{15}N and ^{13}CO magnetisations along the z-axis, significant relaxation losses are not expected in the study of moderately sized proteins. Considering that neither non-optimal delays nor inefficient magnetisation transfer types were required to achieve sequential data acquisition, the signal to noise ratio observed in the sequentially acquired correlation spectra is not expected to be significantly different from that obtained in stand alone experiments. Even if the signal to noise ratio observed in the spectra following the second sequential ^{1}H acquisition is slightly less than what could be obtained in a stand alone experiment, we are sure that it is advantageous

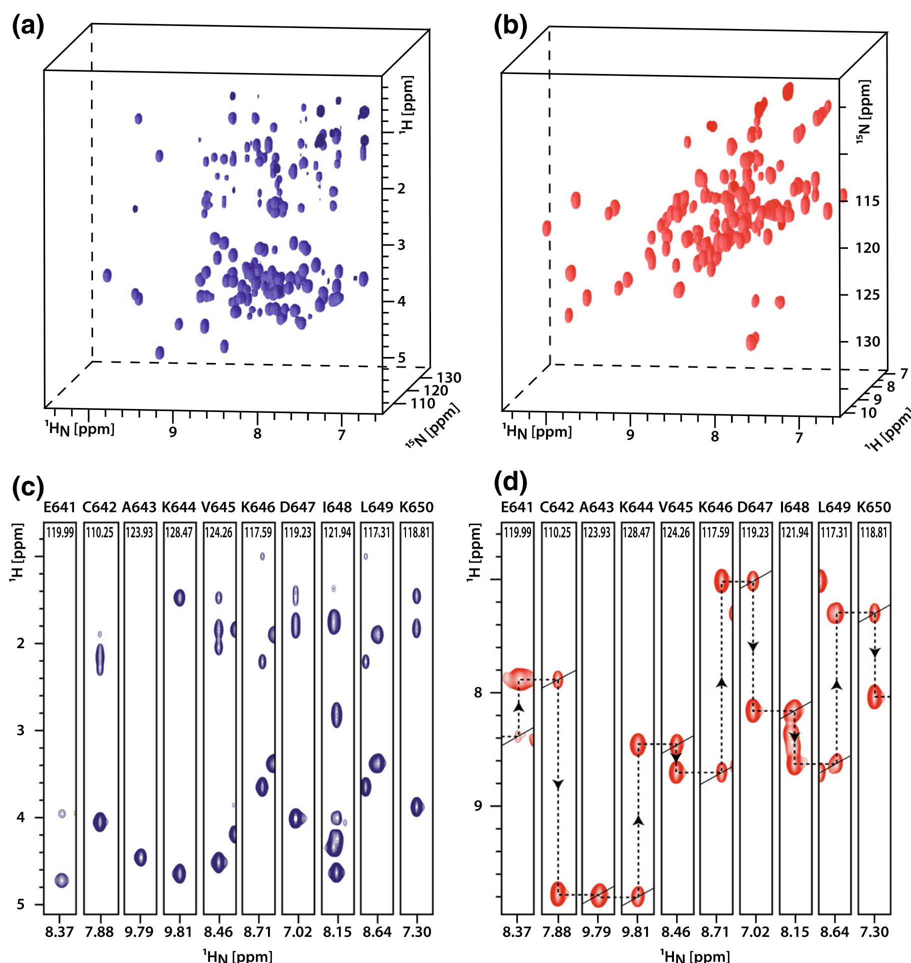

Fig. 2 Simultaneously acquired (**a**) 3D H(CCCO)NH and (**b**) 3D H(NCOCA)NH spectra of MCM C- terminal WH domain recorded at 750 MHz with 16 transients per t_1 increment, 56 t_1 increments, 40 t_2 increments, spectral widths in the indirect dimensions of 4,501 Hz (^{1}H) and 2,737 Hz (^{15}N), a recycle time of 1.0 s and a proton acquisition time in the direct dimension of 60 ms. The total experimental time was ≈55 h. The AK2-JCC and AK4-JC$^{\alpha}$C$'_{aniso}$ sequences reported (Kirschstein et al. 2008a, b) were used, respectively, for ^{13}C-^{13}C isotropic mixing and ^{13}C$^{\alpha}$-^{13}CO anisotropic cross polarisation. The ^{13}C-^{13}C mixing was carried out keeping the ^{13}C RF carrier at 35 ppm, with a peak RF power level of ≈ 10 kHz and for a total duration of 9.6 ms by repeating the basic sequence twice (4.8 ms * 2). The ^{13}C$^{\alpha}$-^{13}CO mixing was carried out keeping the ^{13}C RF carrier at 115 ppm, with a peak RF power level of ≈12 kHz and for a total duration of 18 ms by repeating the basic sequence twice (6 ms * 3). The ^{1}H RF carrier was kept at 3 ppm during t_1 and switched back to the water position (4.7 ppm) after that. (**c**, **d**) ^{1}H^N $-^1$ H^N spectral cross-sections from the H(CCCO)NH (*blue*) and H(NCOCA)NH (*red*) spectra taken at the ^{15}N chemical shifts positions indicated and showing the sequential walk along the backbone residues spanning the region E641-K650

to exploit the sequential data acquisition procedure to minimise spectral data acquisition time, especially in situations where long term stability of a protein sample is a limiting factor.

Our earlier studies (Bellstedt et al. 2014; Wiedemann et al. 2014), carried out at 600 MHz, made use of a ^{15}N-^{13}C het-TOCSY mixing step as one of the building blocks of the RF pulse scheme. However, application of het-TOCSY mixing schemes over long periods of time can lead to excessive sample heating and may pose problems for the study of temperature sensitive samples. Therefore, the pulse schemes, demonstrated here at 750 MHz, have been implemented using only INEPT-type ^{15}N-^{13}C magnetisation transfers. Such transfers, besides minimising sample heating effects, additionally permit simultaneous chemical shift labelling during the ^{15}N-^{13}C magnetisation transfer step and thereby reduce the overall duration of the pulse sequence. The sequences reported here and in our earlier studies have been implemented taking into consideration different factors: the size of the protein to be studied, fully protonated or ^{2}H-labelled sample, type of probe to be employed (cryo- or room temperature probe), and the spectrometer frequency. Hence, the type of sequence to be used in a given situation has to be decided based on these

Fig. 3 Simultaneously acquired **a** 3D (H)C(CCO)NH and **b** 3D (HN)CO(CA)NH spectra of MCM C- terminal WH domain recorded at 750 MHz with 16 transients per t_1 increment, 42 t_1 increments, 50 t_2 increments, spectral widths in the indirect dimensions of 2,737 Hz (^{13}CO), 2,737 Hz (^{15}N) and 10,948 Hz ($^{13}C^{sc}$), a recycle time of 1.0 s and a proton acquisition time in the direct dimension of 60 ms. The total experimental time was $\approx$ 51 h. $^{13}C-^{13}C$ isotropic and $^{13}C^{\alpha}-^{13}CO$ anisotropic mixings were carried out as in Fig. 2. The ^{1}H RF carrier was kept at 4.7 ppm. **c**, **d** $^{13}C^{sc}$ – $^{1}H^{N}$ and ^{13}CO – $^{1}H^{N}$ spectral cross-sections from the (H)C(CCO)NH (*blue*) and (HN)CO(CA)NH (*red*) spectra taken at the ^{15}N chemical shifts positions indicated and showing the sequential walk along the backbone residues spanning the region E641-K650

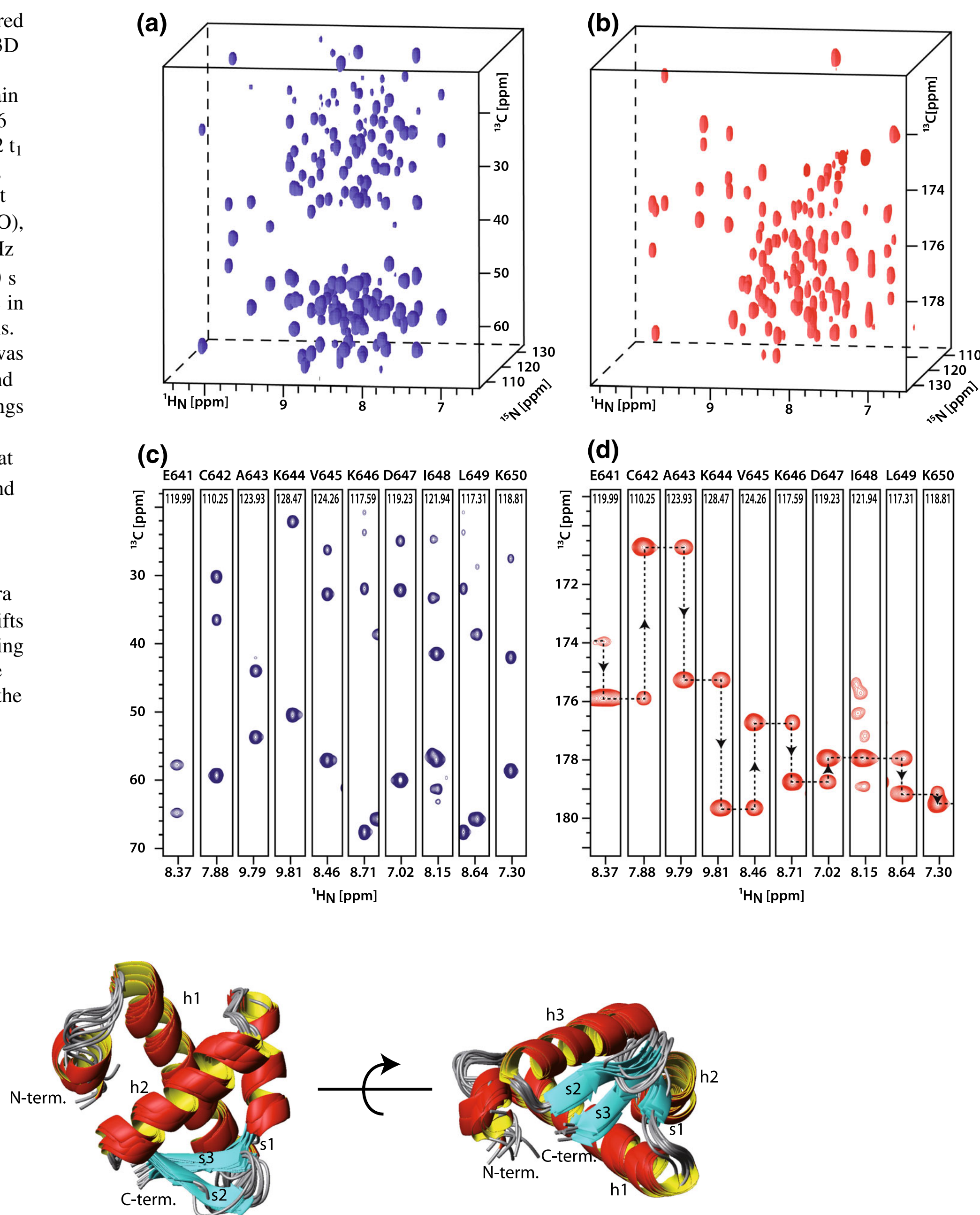

Fig. 4 Superposition of the backbone ribbon representations of ten lowest energy CS-Rosetta structures of the C-terminal winged helix (WH) domain of the MCM complex. The ensemble backbone rmsd to the global mean structure is 1.43 ± 0.37 Å. h1-3: helix, s1-3: sheet

considerations. For example, for a ^{2}H-labelled protein, the RF pulse schemes involving $^{1}H^{\alpha}$ detection either in the direct or indirect dimension (Bellstedt et al. 2014) will not be effective. In situations where the sample concentration is not very high, it may be advantageous to employ sequences based on a single ^{15}N-^{13}C mixing step that have better sensitivity (Bellstedt et al. 2014).

A different approach yielding to sequential resonance assignments and the extraction of chemical shifts for use in protein structure prediction programs has been proposed recently in the literature (Reddy and Hosur 2014). However, this approach involves the generation of initial transverse magnetisation from ^{13}C attached side chain protons only and requires dual receivers for the simultaneous collection of different triple resonance chemical shift correlation spectra employing ^{1}H and ^{13}C detection in the direct dimension. In contrast, our studies clearly demonstrate that it is possible to conveniently implement RF pulse schemes using sequential data acquisition procedures to achieve simultaneous acquisition of triple resonance

chemical shift correlation spectra of proteins in situations where sensitivity is limited, *e.g.* , when the solution state NMR probe is optimised for ^{1}H detection only, or when dual receiver hardware capabilities are not available.

The presented procedure of sequential data acquisition provides an alternative approach to the well established single triple resonance experiments (*e.g.* HNCACB, HNCO/HN(CA)CO) for achieving chemical shift assignment.

Acknowledgments We thank Thomas Seiboth for helpful discussions during the preparation of the manuscript. CW and PB were supported by the Leibniz Graduated School on Ageing and Age-Related Diseases (LGSA). The FLI is a member of the Science Association 'Gottfried Wilhelm Leibniz' (WGL) and is financially supported by the Federal Government of Germany and the State of Thuringia.

References

Bellstedt P, Ihle Y, Wiedemann C, Kirschstein A, Herbst C, Görlach M, Ramachandran R (2014) Sequential acquisition of multi-dimensional heteronuclear chemical shift correlation spectra with (1)H detection. Sci Rep 4:4490

Bracken C, Palmer AG, Cavanagh J (1997) (H)N(COCA)NH and HN(COCA)NH experiments for 1H–15N backbone assignments in 13C/15N-labeled proteins. J Biomol NMR 9(1):94–100

Brünger AT, Adams PD, Clore GM, DeLano WL, Gros P, Grosse-Kunstleve RW, Jiang JS, Kuszewski J, Nilges M, Pannu NS, Read RJ, Rice LM, Simonson T, Warren GL (1998) Crystallography & NMR system: a new software suite for macromolecular structure determination. Acta Crystallogr D Biol Crystallogr 54(Pt 5):905–921

Carlomagno T, Maurer M, Sattler M, Schwendinger MG, Schwendinger MG, Glaser SJ, Glaser SJ, Griesinger C, Griesinger C (1996) PLUSH TACSY: homonuclear planar TACSY with two-band selective shaped pulses applied to Ca, C' transfer and Cb, caromatic correlations. J Biomol NMR 8(2):161–170

Clowes RT, Boucher W, Hardman CH, Domaille PJ, Laue ED (1993) A 4D HCC(CO)NNH experiment for the correlation of aliphatic side-chain and backbone resonances in 13C/15N-labelled proteins. J Biomol NMR 3(3):349–354

Farmer BT, Venters RA (1995) Assignment of side-chain 13c resonances in perdeuterated proteins. J Am Chem Soc 117(14):4187–4188. doi:10.1021/ja00119a042

Grzesiek S, Anglister J, Ren H, Bax A (1993) 13C line narrowing by 2H decoupling in 2H/13C/15N-enriched proteins. Application to triple resonance 4D J connectivity of sequential amides. J Am Chem Soc 115(10):4369–4370

Güntert P (2004) Automated NMR structure calculation With CYANA. Protein NMR techniques. Humana Press, New Jersey, pp 353–378

Kirschstein A, Herbst C, Riedel K, Carella M, Leppert J, Ohlenschläger O, Görlach M, Ramachandran R (2008a) Broadband homonuclear TOCSY with amplitude and phase-modulated RF mixing schemes. J Biomol NMR 40(4):227–237

Kirschstein A, Herbst C, Riedel K, Carella M, Leppert J, Ohlenschläger O, Görlach M, Ramachandran R (2008b) Heteronuclear J cross-polarisation in liquids using amplitude and phase modulated mixing sequences. J Biomol NMR 40(4):277–283

Lange OF, Baker D (2012) Resolution-adapted recombination of structural features significantly improves sampling in restraint-guided structure calculation. Proteins 80(3):884–895

Lange OF, Rossi P, Sgourakis NG, Song Y, Lee HW, Aramini JM, Ertekin A, Xiao R, Acton TB, Montelione GT, Baker D (2012) Determination of solution structures of proteins up to 40 kDa using CS-Rosetta with sparse NMR data from deuterated samples. Proc Natl Acad Sci USA 109(27):10,873–10,878

Logan TM, Olejniczak ET, Xu RX, Fesik SW (1992) Side chain and backbone assignments in isotopically labeled proteins from two heteronuclear triple resonance experiments. FEBS Lett 314(3):413–418

Morris GA, Freeman R (1979) Enhancement of nuclear magnetic resonance signals by polarization transfer. J Am Chem Soc 101(3):760–762

Raman S, Lange OF, Rossi P, Tyka M, Wang X, Aramini J, Liu G, Ramelot TA, Eletsky A, Szyperski T, Kennedy MA, Prestegard J, Montelione GT, Baker D (2010) NMR structure determination for larger proteins using backbone-only data. Science 327(5968):1014–1018

Reddy JG, Hosur RV (2014) Complete backbone and DENQ side chain NMR assignments in proteins from a single experiment: implications to structure-function studies. J Struct Funct Genomics 15(1):25–32

Schot G, Zhang Z, Vernon R, Shen Y, Vranken WF, Baker D, Bonvin AMJJ, Lange OF (2013) Improving 3D structure prediction from chemical shift data. J Biomol NMR 57(1):27–35

Shen Y, Lange O, Delaglio F, Rossi P, Aramini JM, Liu G, Eletsky A, Wu Y, Singarapu KK, Lemak A, Ignatchenko A, Arrowsmith CH, Szyperski T, Montelione GT, Baker D, Bax A (2008) Consistent blind protein structure generation from NMR chemical shift data. Proc Natl Acad Sci USA 105(12):4685–4690

Shen Y, Delaglio F, Cornilescu G, Bax A (2009) TALOS+: a hybrid method for predicting protein backbone torsion angles from NMR chemical shifts. J Biomol NMR 44(4):213–223

Shirakawa M, Wälchli M, Shimizu M, Kyogoku Y (1995) The use of heteronuclear cross-polarization for backbone assignment of (2)H-, (15)N- and (13)C-labeled proteins: A pulse scheme for triple-resonance 4D correlation of sequential amide protons and (15)N. J Biomol NMR 5(3):323–326

States DJ, Haberkorn RA, Ruben DJ (1982) A two-dimensional nuclear overhauser experiment with pure absorption phase in four quadrants. J Magn Reson 48(2):286–292

Venters RA, Farmer BT, Fierke CA, Spicer LD (1996) Characterizing the use of perdeuteration in NMR studies of large proteins: 13C, 15N and 1H assignments of human carbonic anhydrase II. J Mol Biol 264(5):1101–1116

Wiedemann C, Ohlenschläger O, Medagli B, Onesti S, Görlach M (2013) (1)H, (15)N and (13)C chemical shift assignments for the winged helix domains of two archeal MCM C-termini. Biomol NMR Assign

Wiedemann C, Bellstedt P, Kirschstein A, Häfner S, Herbst C, Görlach M, Ramachandran R (2014) Sequential protein NMR assignments in the liquid state via sequential data acquisition. J Magn Reson 239:23–28

Yamazaki T, Lee W, Arrowsmith CH, Muhandiram DR, Kay LE (1994) A suite of triple resonance NMR experiments for the backbone assignment of 15N, 13C, 2H labeled proteins with high sensitivity. J Am Chem Soc 116(26):11,655–11,666

Zuiderweg EP, Zeng L, Brutscher B, Morshauser R (1996) Band-selective hetero- and homonuclear cross-polarization using trains of shaped pulses. J Biomol NMR 8(2):147–160